Definition of electron temperature of nonequilibrium plasma based on Tsallis and Rényi entropy maximization principles

Koji Kikuchi [1] and Hiroshi Akatsuka [2]

[1]*Graduate Major in Nuclear Engineering, Department of Electrical and Electronic Engineering, Institute of Science Tokyo, 2-12-1-N1-10, O-Okayama, Meguro-ku, Tokyo 152-8550, Japan*

[2]*Institute of Integrated Research, Institute of Science Tokyo, 2-12-1-N1-10, O-Okayama, Meguro-ku, Tokyo 152-8550, Japan*

(Received 8 February 2025; accepted 22 May 2025; published 7 July 2025)

Nonequilibrium plasma has attracted significant attention owing to its excellent physical properties, which are highly valued by the industrial community. However, determining the electron temperature in nonequilibrium plasmas proves challenging unless the energy distribution function is approximated as an ideal Maxwell-Boltzmann distribution, where the slope of the Boltzmann plot is directly related to temperature based on traditional Boltzmann-Gibbs statistics. To overcome this problem, Tsallis and Rényi entropies are applied to nonequilibrium systems using nonextensive Tsallis and extensive Rényi statistics, respectively. Here, the temperature is determined through a power-law distribution derived from the entropy maximization principle, which accounts for the influence of previously neglected high-energy electrons. However, because the resulting distribution function requires a self-consistent function that cannot be solved analytically, a self-consistent iterative scheme is proposed to calculate the temperature. Consequently, the electron temperature is uniquely determined in nonequilibrium plasmas, satisfying the entropy maximization principle. This study may open additional avenues for understanding plasma properties using an additional parameter q expanding the meaning of temperature T.

DOI: 10.1103/6zfg-q1b9

I. INTRODUCTION

The dynamics of a physical system at equilibrium is governed by the entropy maximization principle in conventional statistical physics [1]. However, dynamic systems comprising multibody Coulomb collision, radiation, absorption, excitation, drift, or diffusion processes, such as the physical ones associated with plasmas, often deviate from the traditional Gibbs entropy maximization principle that is considered the ideal state in standard statistical mechanics [2–4].

In plasma physics, numerous studies have suggested that the statistical properties of nonequilibrium plasmas often diverge from the canonical Maxwell-Boltzmann distributions owing to their nonequilibrium characteristics. Specifically, the high-energy tail of these energy distribution becomes either rich [5–12] or depleted [13–19], depending on the underlying elementary processes of plasmas. For example, magnetic reconnection in the Earth's magnetosphere causes population inversion that becomes convex downward on a semi-logarithmic scale [5,6]. In contrast, in atmospheric-pressure nonequilibrium discharge plasma, the electron energy distribution function (EEDF) becomes convex upward as the electrons accelerated by the electric field fail to reach thermodynamic equilibrium with atoms or ions, particularly when their collision frequencies are low. Consequently, researchers often approximate the electron energy distribution as an empirically derived Druyvesteyn distribution, where the population is proportional to the modified Boltzmann factor whose characteristics are proportional to the square of the energy [13,18].

This deviation from the Maxwell-Boltzmann distribution causes problems in determining the temperature of each system. To uniquely determine the temperature of each dynamical system, its distribution function must be approximated to the Maxwell-Boltzmann distribution [18,19] within the framework of traditional Boltzmann-Gibbs statistics, where the slope of the Boltzmann plot is directly related to the temperature, as follows:

$$p_i \propto \exp\left(-\frac{E_i}{kT}\right), \tag{1}$$

where p_i is the probability that the system is in the ith state, E_i is the energy of the ith level, k is the Boltzmann constant, and T is the temperature. The Boltzmann plot obtained by plotting p_i semi-logarithmically against E_i exhibits a straight line in the equilibrium state. However, some approximations are required to describe the nonequilibrium state temperature because the temperature inferred from the slope of the high-energy region differs from that at the low-energy region, as shown in the Boltzmann plot in Fig. 1. As a result, the temperature derived from the Boltzmann plot, the partial derivative of entropy, and the mean energy cannot coexist within conventional Boltzmann-Gibbs statistics.

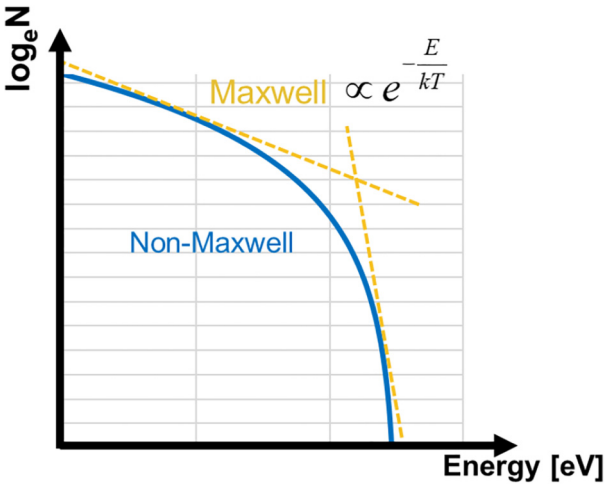

FIG. 1. Schematic example of Boltzmann plot comparing Maxwellian and non-Maxwellian distribution functions. The temperature inferred from the slope in the high-energy region differs from that in the low-energy region.

The temperatures of nonequilibrium plasma, which do not obey the Maxwell-Boltzmann distribution, were determined using the Boltzmann plot [20–22] or the mean energy calculations [23–27]. However, these temperature measures did not mathematically coincide under the non-Maxwell-Boltzmann distribution. Therefore, new approaches using the concept of entropy were proposed [28–30]. The temperature of out-of-equilibrium free electrons in cold plasmas was successfully calculated based on Gibbs statistics [28,29]. These theories can be used to calculate the partial derivative of the conventional Gibbs entropy with respect to the mean energy of the electrons as follows:

$$T_{\mathrm{Gibbs}} = \left(\frac{\partial s}{\partial u}\right)^{-1}, \tag{2}$$

which almost corresponds to the effective temperature T_{eff}, given as

$$T_{\mathrm{eff}} = \frac{2u}{3k} = \frac{2}{3k}\int_0^\infty \epsilon f(\epsilon)\mathrm{d}\epsilon, \tag{3}$$

where ϵ and $f(\epsilon)$ are the electron energy and EEDF, respectively. However, Eq. (2) derived from Boltzmann-Gibbs statistics is unsuitable for dynamic systems owing to the failure to satisfy the entropy maximization principle. Because of the Gibbs entropy maximization, Eq. (2) must hold the exponential energy distribution function [31]. Consequently, the two temperatures derived from Gibbs statistics cannot coexist under realistic conditions [29].

To overcome this problem, we apply nonextensive Tsallis and extensive Rényi statistics to nonequilibrium systems. Tsallis and Rényi entropies are generalizations of Gibbs entropy [32,33], mathematically transforming the exponential distribution into power-law distributions. The traditional Gibbs entropy is exactly recovered in the limit $q \to 1$. This property of power-law functions describes nonequilibrium characteristics containing rich or depleted high-energy tails, corresponding to applying nonextensive Tsallis and extensive Rényi statistics. However, because the resulting electron energy distribution function requires a self-consistent function that cannot be solved analytically, a self-consistent iterative scheme is proposed to calculate the temperature. Furthermore, because the electron energy distribution in plasma is continuous, the direct application of the inherently discrete nonextensive Tsallis and extensive Rényi statistics is inappropriate. Therefore, we define the Tsallis and Rényi differential entropy using the electron energy probability function in plasma to calculate the Tsallis and Rényi temperatures.

As described above, in the nonequilibrium state, the temperature is determined based on the slope of the distribution function or the mean energy of each dynamic system [20–27]. However, the system entropy can be calculated directly from the distribution function without using equilibrium concepts such as "free energy" [28–30]. We have applied Tsallis entropy to the excitation distribution, which follows a discrete distribution [30]. In this study, we focus on the temperatures from the application of Tsallis and Rényi entropies to EEDF, which follows a continuous distribution. To apply Tsallis and Rényi statistics to EEDF, Tsallis and Rényi statistics are redefined using the continuous distribution in Sec. II D. Furthermore, we discuss their implications. Both entropies exhibit distinct characteristics in the high-energy region of distributions, with their curvatures exhibiting opposing behavior. This approach enables the calculation of the temperature based on the principles of statistical physics. Accordingly, the present study redefines "electron temperature" in nonequilibrium plasma systems exhibiting non-Maxwell-Boltzmann distributions from the perspectives of extended extensive and nonextensive statistical physics individually. This approach can potentially open additional research avenues because current conventional methods for determining temperature often overlook the curvilinear distribution of the high-energy tail in plasma physics. Therefore, by incorporating the parameter q alongside the temperature T within the framework of the Tsallis and Rényi entropy maximization principles, a more comprehensive description of the plasma's properties can be obtained.

Additionally, numerous studies have explored the application of Tsallis and Rényi entropies to several physical systems. One such study was conducted to derive entropy with the same physical significance as Tsallis entropy, as well as the q-exponential form, based on the number of weighted microstates of the phase space [34]. In contrast, our research focuses on distributions governed by entropy maximization conditions, which require specialized self-referential functions. Moreover, by calculating temperature as the partial derivative of Tsallis and Rényi entropies with respect to the average energy, we demonstrate the differences in temperature in Tsallis and Rényi statistics frameworks and discuss the validity and appropriateness of applying these types of entropy.

II. THEORETICAL BACKGROUNDS

In statistical physics, researchers developed mathematical frameworks to explain observed distribution functions that traditional statistical principles cannot account for [32,33,35–39]. In particular, in extended extensive and

nonextensive statistical physics, Tsallis entropy [32] and Rényi entropy [33] serve as one-parameter extensions that reflect the degree of departure from Boltzmann-Gibbs statistics. These entropies agree with the traditional Gibbs entropy in the limit $q \to 1$. These methods enable the description of its entropy, which fundamentally follows a power-law distribution instead of a traditional exponential distribution. Thus, this approach facilitates describing the distributions observed in various systems, which cannot be derived through ordinary statistical mechanics. Consequently, Tsallis entropy [40–48] and Rényi entropy [49–55] were applied to various nonequilibrium phenomena across multiple fields of physics.

A. Tsallis statistics

This subsection demonstrates that the probability function should be followed by the q-exponential distribution function to determine the temperature derived from Tsallis statistics. By adopting the maximum entropy principle in Tsallis statistics, as in Boltzmann-Gibbs statistics, the unique self-referential q-exponential distribution function can be derived [56,57]. Tsallis statistics is extended by satisfying the constraint conditions in Eq. (4) and the following two conditions for the total number of microscopic possibilities of the system W and the q-average energy U_q :

$$S_{\text{Tsallis}} = -k\frac{\sum_{i=1}^{W} p_i^q - 1}{q-1}, \tag{4}$$

$$\sum_{i=1}^{W} p_i = 1, \tag{5}$$

and

$$U_q = \frac{\sum_{i=1}^{W} p_i^q \epsilon_i}{\sum_{j=1}^{W} p_j^q}, \tag{6}$$

where S_{Tsallis} is the Tsallis entropy and ϵ_i is the energy at level i. By selecting U_q instead of conventional mean energy, the macroscopic additivity of U_q is preserved in accordance with the first principle of thermodynamics (energy conservation). Furthermore, Legendre transformation, an involution transformation commonly used in thermodynamics, is satisfied even in Tsallis statistics [56]. Under the condition of maximizing Tsallis entropy using the Lagrange multiplier method, this probability function can be derived as

$$p_i = \frac{1}{Z_q(\beta)}[1 - \beta_q(1-q)(\epsilon_i - U_q)]^{\frac{1}{1-q}}. \tag{7}$$

Unlike the exponential probability function in Gibbs statistics, Eq. (7) determines a self-consistent function p_i appearing on both sides, which cannot be solved analytically. $Z_q(\beta)$ is the generalized partition function given as

$$Z_q(\beta) = \sum_{i=1}^{W}[1 - \beta_q(1-q)(\epsilon_i - U_q)]. \tag{8}$$

In contrast, β_q is defined as

$$\beta_q = \frac{q}{q + (1+\alpha)(1-q)}\beta, \tag{9}$$

where α and β are Lagrange multipliers associated with the normalization constraint. Because β_q is regarded as an energy coefficient, the temperature $T_{\beta-\text{Tsallis}}$ in Tsallis statistics is defined as

$$T_{\beta-\text{Tsallis}} = \frac{1}{k\beta_q}. \tag{10}$$

The obtained $T_{\beta-\text{Tsallis}}$ coincides with the physical temperature derived in accordance with the zeroth law of thermodynamics [58]

$$T_{q-\text{Tsallis}} = \left(1 + \frac{1-q}{k}S_q\right)\left(\frac{\partial S_{\text{Tsallis}}}{\partial U_q}\right)^{-1}. \tag{11}$$

Therefore, these temperatures are referred to as the Tsallis temperature T_{Tsallis}. Equations (10) and (11) hold true when the probability function is governed by Eq. (7). In addition, we define the temperature

$$T_{U_q-\text{Tsallis}} \equiv \frac{U_q}{k}, \tag{12}$$

derived from the q-average energy, which corresponds to its analogy in Gibbs statistics [30].

B. Rényi statistics

This subsection demonstrates that the probability function should be followed by the Rényi distribution function, which exhibits a power-law function similar to that derived from Tsallis statistics. This property facilitates determination of the temperature within the Rényi statistics framework. By adopting the maximum entropy principle in Rényi statistics, a self-referential power-law distribution function that maintains duality with Tsallis statistics can be derived, similar to that used in Tsallis statistics [59–61]. Rényi statistics is extended by satisfying the constraint conditions Eqs. (13) and (5) and the following condition on the total number of microscopic possibilities of system W and mean energy:

$$S_{\text{Rényi}} = k\frac{\ln\sum_{i=1}^{W} p_i^q}{1-q}, \tag{13}$$

$$U = \sum_{i=1}^{W} p_i \epsilon_i. \tag{14}$$

By maximizing the Rényi entropy using the Lagrange multiplier method, this probability function can be derived as follows:

$$p_i = \frac{1}{Z'_q(\beta)}\left[1 - \beta\frac{q-1}{q}(\epsilon_i - U)\right]^{\frac{1}{q-1}}. \tag{15}$$

Similar to Tsallis statistics, p_i is obtained using Eq. (15) as a self-referential function, which cannot be solved analytically. $Z_q(\beta)$ is the generalized partition function

$$Z'_q(\beta) = \sum_{i=1}^{W}\left[1 - \beta\frac{q-1}{q}(\epsilon_i - U)\right]. \tag{16}$$

Additionally, $T_{\beta-\text{Rényi}}$ is defined as

$$T_{\beta-\text{Rényi}} = \frac{1}{k\beta}. \tag{17}$$

The obtained $T_{\beta-\text{Rényi}}$ matches the temperature derived from the partial derivative of the Rényi entropy with respect to the mean energy, in accordance with the zeroth law of thermodynamics [60]

$$T_{q-\text{Rényi}} = \left(\frac{\partial S_{\text{Rényi}}}{\partial U}\right)^{-1}. \tag{18}$$

Furthermore, these temperatures coincide with those derived from the mean energy U [59]

$$T_{U-\text{Rényi}} = \frac{U}{k}. \tag{19}$$

Consequently, the three temperatures in Eqs. (17)–(19) coincide with Rényi statistics and are called the Rényi temperatures $T_{\text{Rényi}}$. Eqs. (17)–(19) hold when the probability function is given by the power-law function Eq. (15).

C. Electron energy distribution in gas discharge plasma using Boltzmann equation

The Boltzmann equation, developed by Boltzmann in 1872, describes the statistical behavior of nonequilibrium thermodynamic systems [62]. Based on the Boltzmann equation, the Maxwell-Boltzmann distribution can be derived as a stationary solution when the detailed balance and spatial uniformity conditions hold and there are no external forces. The EEDF of the fluid-model gas discharge plasma can be calculated by solving the Boltzmann equation using the fundamental collision cross-section data. This equation describes the transport of electrons, ions, and possibly other reactive particle species.

We employ BOLSIG+, a two-term Boltzmann solver, which utilizes updated cross-section data from the LXcat database to solve the Boltzmann equation. These data encompass elastic collisions, symmetrical vibrational excitation, electronic excitation, and ionization cross sections [63]. Numerous studies assessed the cross section for momentum transfer, electronic excitation, and the ionization of noble gases [64–66]. In this study, the argon cross section set provided by ISTLISBON, comprising 39 cross sections (including elastic momentum-transfer, 37 excitations, and ionization) up to 1 keV, is employed [64,67–76]. It was reported that when these cross sections are used as input data in a two-term Boltzmann solver that the resulting swarm parameters generally agree with experimental measurements. The solver provides steady-state solutions to the Boltzmann equation for electrons in uniform electric fields using a classical two-term expansion. In addition, it can account for different growth models, quasistationary and oscillating fields, electron-neutral collisions, and electron-electron collisions.

The evolution of the distribution function $f(v)$ is as follows:

$$\frac{\partial f}{\partial t} + \boldsymbol{v}\cdot\nabla f + \frac{e\boldsymbol{E}}{m_e}\cdot\frac{\partial f}{\partial \boldsymbol{v}} = \left(\frac{\delta f}{\delta t}\right)_{\text{coll}}, \tag{20}$$

where $\boldsymbol{E}$ is the electric field acting on the particles in the fluid and $(\delta f/\delta t)_{\text{coll}}$ is the collision term. The time derivative of the distribution function incorporates force, diffusion, and collision terms. By contrast, the distribution function $f(v)$ can be expanded in spherical harmonics. In solving partial differential equations, a two-term approximation of $f(v)$ under an external electric field along the velocity vector in the z axis is often employed

$$f(\boldsymbol{v}) = f_0(\boldsymbol{v}) + \frac{v_z}{v} f_1(\boldsymbol{v}), \tag{21}$$

where f_0 is the isotropic part of $f(v)$ and f_1 is an anisotropic perturbation [77–79]. Additionally, electrons do not depend on the spatial coordinates $\nabla = 0$ at the collisional mean-free path scale in the symmetric velocity space along the electric field direction. Therefore, $f(\boldsymbol{v})$ can be equivalently expressed as $f(v)$, indicating a scalar velocity function.

The Maxwellian EEDF for electrons is described as follows [80]:

$$f_{\text{M}}(\epsilon) = \frac{2}{\sqrt{\pi}}\left(\frac{1}{kT_{\text{e}}}\right)^{3/2}\exp\left(-\frac{\epsilon}{kT_{\text{e}}}\right)\sqrt{\epsilon}, \tag{22}$$

which are valid only under equilibrium conditions. The EEDF is characterized by Boltzmann factor $\exp[-\epsilon/(kT_e)]$ with weighting factor $\sqrt{\epsilon}$. Therefore, many studies applied the EEPF

$$F(\epsilon) = \frac{f(\epsilon)}{\sqrt{\epsilon}}, \tag{23}$$

to discuss the properties of plasma [81–83] as the Boltzmann plot becomes linear against the Maxwellian EEDF. In plasma physics, various studies applied EEPF by solving the Boltzmann equation as a function of the reduced electric field E/N, where N denotes the number density of neutral particles.

D. Application and adaptation of nonextensive Tsallis and extensive Rényi statistics: A fitting approach

To describe the entropy of systems using nonextensive Tsallis and extensive Rényi statistics, the distribution function should be fitted using Tsallis or Rényi distributions, as shown in Eqs. (7) and (15), respectively. However, because the electron energy distribution in plasma is continuous, the direct application of the inherently discrete nonextensive Tsallis and extensive Rényi statistics is inappropriate. Shannon extended his entropy concept, which was originally defined for discrete probability distributions, to continuous systems through differential entropy [84]. Following this analogy, Tsallis differential entropy [85] and Rényi differential entropy [86] emerged. Both differential entropies are defined using EEPF in plasma as

$$s_{\text{Tsallis}} = -k\frac{\int_{\mathcal{X}} F^q(\epsilon)\mathrm{d}\epsilon - 1}{q-1}, \tag{24}$$

$$s_{\text{Rényi}} = k\frac{\ln\int_{\mathcal{X}} F^q(\epsilon)\mathrm{d}\epsilon}{1-q}, \tag{25}$$

where $\mathcal{X}$ is the support of the set of energies ϵ. Similarly, to determine the effect of temperature on the nonextensive

TABLE I. Iterative scheme to solve self-referential function.

Tsallis	Rényi
1: Initialize	1: Initialize
$z_{q(0)}(\beta) = \int_{\mathcal{X}} [1 - \beta_q(1-q)\epsilon]\mathrm{d}\epsilon$	$z'_{q(0)}(\beta) = \int_{\mathcal{X}} \left(1 - \beta\frac{q-1}{q}\epsilon\right)\mathrm{d}\epsilon$
$F_{(0)}(\epsilon) = \frac{1}{z_{q(0)}(\beta)}[1 - \beta_q(1-q)\epsilon]^{\frac{1}{1-q}}$	$F_{(0)}(\epsilon) = \frac{1}{z'_{q(0)}(\beta)}\left(1 - \beta\frac{q-1}{q}\epsilon\right)^{\frac{1}{q-1}}$
$u_{q(0)} = \frac{\int_{\mathcal{X}} F^q_{(0)}(\epsilon)\epsilon\mathrm{d}\epsilon}{\int_{\mathcal{X}} F^q_{(0)}(\epsilon)\mathrm{d}\epsilon}$	$u_{(0)} = \int_{\mathcal{X}} F_{(0)}(\epsilon)\epsilon\mathrm{d}\epsilon$
2: Iterate $k = 0, 1, 2, \ldots,$ until convergence	2: Iterate $k = 0, 1, 2, \ldots,$ until convergence
$z_{q(k+1)}(\beta) = \int_{\mathcal{X}} [1 - \beta_q(1-q)(\epsilon - u_{q(k)})]\mathrm{d}\epsilon$	$z'_{q(k+1)}(\beta) = \int_{\mathcal{X}} \left[1 - \beta\frac{q-1}{q}(\epsilon - u_{(k)})\right]\mathrm{d}\epsilon$
$F_{(k+1)}(\epsilon) = \frac{1}{z_{q(k+1)}(\beta)}[1 - \beta_q(1-q)(\epsilon - u_{q(k)})]^{\frac{1}{1-q}}$	$F_{(k+1)}(\epsilon) = \frac{1}{z'_{q(k+1)}(\beta)}\left[1 - \beta\frac{q-1}{q}(\epsilon - u_{(k)})\right]^{\frac{1}{q-1}}$
$u_{q(k+1)} = \frac{\int_{\mathcal{X}} F^q_{(k+1)}(\epsilon)\epsilon\mathrm{d}\epsilon}{\int_{\mathcal{X}} F^q_{(k+1)}(\epsilon)\mathrm{d}\epsilon}$	$u_{(k+1)} = \int_{\mathcal{X}} F_{(k+1)}(\epsilon)\epsilon\mathrm{d}\epsilon$

Tsallis and extensive Rényi statistics, we redefine Eqs. (6)–(8) and (14)–(16) as follows:

$$u_q = \frac{\int_{\mathcal{X}} F^q(\epsilon)\epsilon\mathrm{d}\epsilon}{\int_{\mathcal{X}} F^q(\epsilon)\mathrm{d}\epsilon}, \tag{26}$$

$$F(\epsilon) = \frac{1}{Z_q(\beta)}[1 - \beta_q(1-q)(\epsilon - u_q)]^{\frac{1}{1-q}}, \tag{27}$$

$$z_q(\beta) = \int_{\mathcal{X}} [1 - \beta_q(1-q)(\epsilon - u_q)]\mathrm{d}\epsilon, \tag{28}$$

$$u = \int_{\mathcal{X}} F(\epsilon)\epsilon\mathrm{d}\epsilon, \tag{29}$$

$$F(\epsilon) = \frac{1}{z'_q(\beta)}\left[1 - \beta\frac{q-1}{q}(\epsilon - u_q)\right]^{\frac{1}{q-1}}, \tag{30}$$

$$z'_q(\beta) = \int_{\mathcal{X}} \left[1 - \beta\frac{q-1}{q}(\epsilon - u)\right]\mathrm{d}\epsilon. \tag{31}$$

The distribution function, treated as a continuous distribution, satisfies the equations derived from the extended extensive and nonextensive statistical physics in Eqs. (10)–(12) and (17)–(19). Therefore, Eqs. (11), (12), (18), and (19) are redefined as

$$T_{q-\mathrm{Tsallis}} = \left(1 + \frac{1-q}{k}s_q\right)\left(\frac{\partial s_{\mathrm{Tsallis}}}{\partial u_q}\right)^{-1}, \tag{32}$$

$$T_{u_q-\mathrm{Tsallis}} \equiv \frac{u_q}{k}, \tag{33}$$

$$T_{q-\mathrm{Rényi}} = \left(\frac{\partial s_{\mathrm{Rényi}}}{\partial u}\right)^{-1}, \tag{34}$$

$$T_{u-\mathrm{Rényi}} = \frac{u}{k}. \tag{35}$$

Equations (27) and (30) are self-referencing functions, preventing an analytical solution for the probability distribution. Therefore, a self-consistent iterative scheme is applied, as shown in Table I. This scheme is the same as that adopted in our previous study [30].

The dependence of the power-law distribution functions $F(\epsilon)$(Tsallis) and $F(\epsilon)$(Rényi), defined in Eqs. (27) and (30), respectively, on arguments q_{T} and q_{R} (q parameters in Tsallis and Rényi statistics) are shown in Fig. 2. The Boltzmann plot becomes a straight line as the limit $q \to 1$. In addition, under conditions of maximized entropy, where the probability distribution follows the power law, a decrease in curvature in the region below the black line (indicating an increase in q_{T}) reduces the Tsallis entropy. Conversely, this decrease in curvature in the region below the black line (indicating a decrease in q_{R}) increases Rényi entropy. The relationship between the curvature associated with the q value and the two entropy types is inverse, as illustrated in Fig. 3. Therefore, in cases where the distribution function shows significant variations in q while $1/\beta$ increases minimally, the Rényi entropy is appropriate in terms of entropy's dependence on the q parameter and is governed by elementary processes that the curvature decreases with increasing mean energy. Conversely, in terms of entropy's dependence on the q parameter, it might be assumed that the Tsallis entropy is suitable for distributions such as the excited-state distribution of low-temperature hydrogen plasma [15,87], where the curvature increases with increasing mean energy.

III. RESULTS AND DISCUSSION

A. Electron energy probability function

In this study, we simulate a weakly ionized Ar discharge plasma based on the Boltzmann equation in Sec. II C to investigate the EEPF profile as shown in Fig. 4. The plasma parameters are chosen in accordance with the experimental observations in earlier studies on plasma generated by common discharge devices [88,89]. Figure 4 reveals a curved

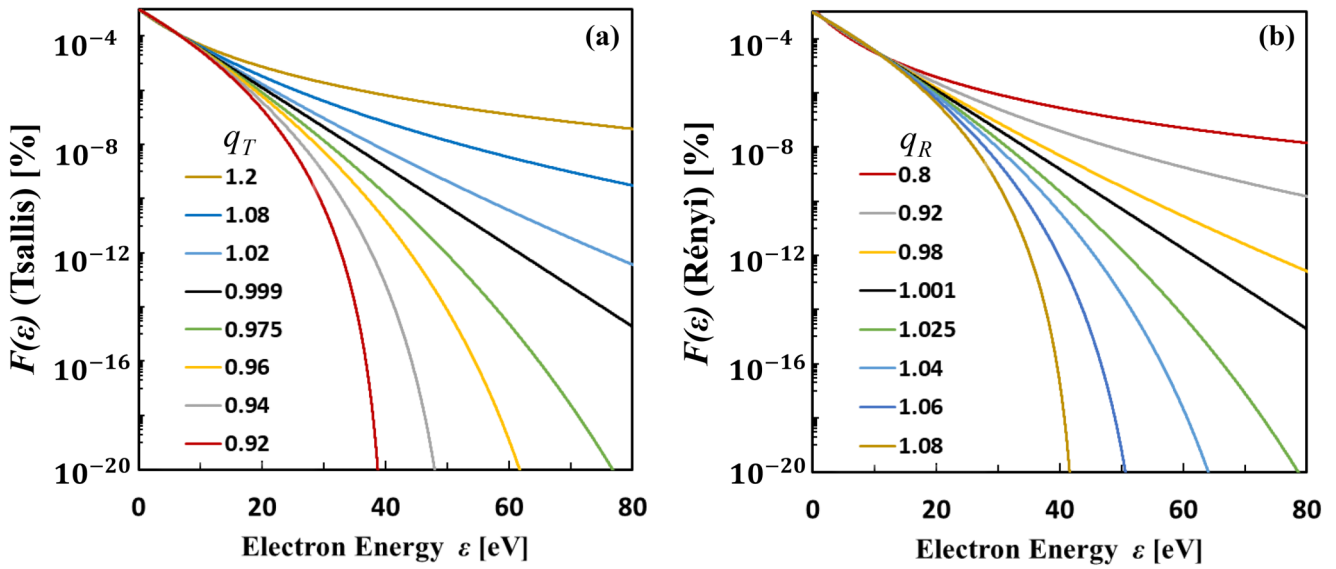

FIG. 2. Schematic of the dependence of the q-exponential distribution function. (a) $F(\epsilon)$(Tsallis) defined in Eq. (27) on parameter q_T, with constant parameters $\alpha = -1$, $1/\beta = 3$. (b) $F(\epsilon)$(Rényi) defined in Eq. (30) on parameter q_R, with constant parameters $1/\beta = 3$.

distribution in the high-energy region, indicating that the EEPF distribution diverges from the Maxwell-Boltzmann profile. This divergence results from the energy dependence of the cross sections of inelastic electron collisions, whereas increasing the electric field generates high-energy electrons in the tail region. These EEPFs indicate that the electron temperature determined from current conventional Gibbs statistics varies depending on the analyzed energy region. For nonextensive Tsallis and extensive Rényi statistics, the distribution function should be fitted by the Tsallis or Rényi distribution to calculate the temperature, respectively, provided that the EEPF is represented by the q distribution. The probability distributions of EEPF $F(\epsilon)$(Tsallis) and $F(\epsilon)$(Rényi) fitted by the Tsallis and Rényi distributions, respectively, are shown in Fig. 5; the specified parameters are listed in Table II. These results demonstrate that $F(\epsilon)$(Tsallis) and $F(\epsilon)$(Rényi) can more accurately describe the curved properties than when applying Gibbs statistics, which yields a straight line. Furthermore, $F(\epsilon)$(Tsallis) and $F(\epsilon)$(Rényi) reproduce nearly the same distribution when the q value is selected appropriately.

B. Tsallis and Rényi entropies

Based on Rényi statistics, the temperature can be derived from the reciprocal of the partial derivative of Rényi entropy with respect to mean energy, similar to that in traditional Boltzmann-Gibbs statistics as described in Eq. (2). In contrast, the temperature in Tsallis statistics is adjusted based on the

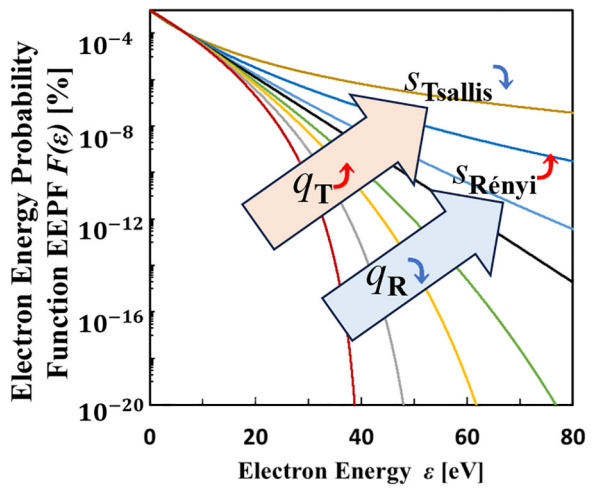

FIG. 3. Schematic of the dependence of the extensive and nonextensive differential entropies on q value. The decrease in curvature in the region below the black line increases q_T and decreases q_R, thereby decreasing Tsallis entropy and increasing Rényi entropy, respectively, for a constant β.

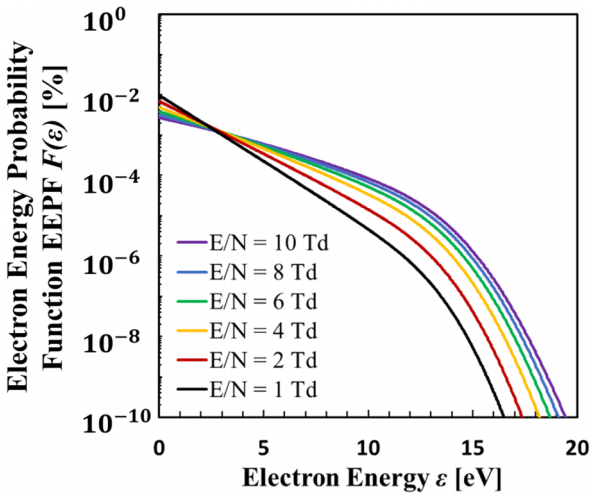

FIG. 4. EEPF of the weakly ionized Ar plasma obtained by the method described in Sec. II D, calculated using BOLSIG+ [63] under the following conditions: gas temperature $T_g = 0.026$ eV, electron density $n_e = 2 \times 10^{13}$ cm^{-3}, and ionization degree 0.012%, for reduced electric field range $1 \leqslant E/N$ [Td] $\leqslant 10$.

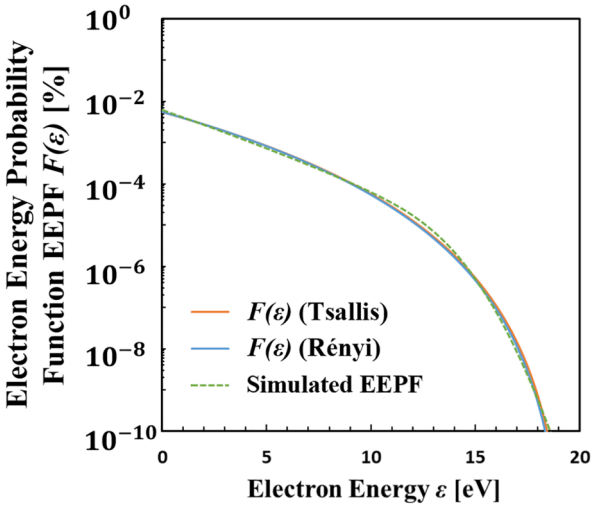

FIG. 5. Fitting curve of the probability distribution of the EEPF of the weakly ionized Ar plasma at reduced electric field $E/N = 5$ Td using the best fitting parameters of Tsallis distribution $F(\epsilon)$(Tsallis) with $q_T = 0.845$ and Rényi distribution $F(\epsilon)$(Rényi) with $q_R = 1.154$. Other plasma parameters are chosen to be the same as in Fig. 4.

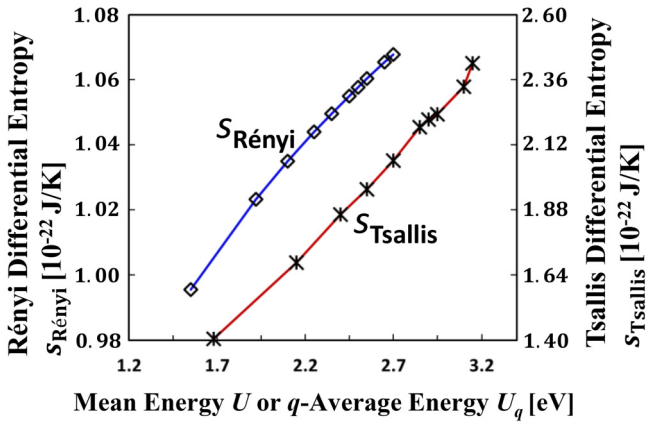

FIG. 6. Tsallis differential entropy versus q-average energy and Rényi differential entropy versus mean energy. The plasma parameters are chosen to be the same as in Fig. 4, scanned within the range of the reduced electric field from $1 \leqslant E/N$ [Td] $\leqslant 10$.

q value, as described in Eq. (11). In Fig. 6, the relationship between Tsallis differential entropy [Eq. (24)] and q-average energy [Eq. (26)] is shown in red, whereas that between the Rényi differential entropy [Eq. (25)] and mean energy [Eq. (29)] is shown in blue.The Tsallis and Rényi differential entropies increase with increasing q average and mean energy, respectively. Although a decrease in curvature (increase in q_T) typically causes the Tsallis differential entropy to decrease, the increase in this case is due to the significant variation in $1/\beta$ with changes in curvature.

Notably, the thermodynamic stability conditions should require the concave entropy function. It was reported that Tsallis and Rényi entropies fail to fulfill the condition of concavity for $q > 1$ [90], and when entropy exhibits concavity, the system's heat capacity is found to become negative. However, in certain types of black holes, including Schwarzschild holes, the entropy is not necessarily required to be concave for thermodynamic stability under specific conditions [91]. Moreover, negative heat capacity was reported in high-temperature hydrogen plasma waves [92]. This highlights the necessity of carefully choosing Tsallis and Rényi temperatures to match specific physical systems. In the plasma system investigated in this study, the simulations demonstrate thermodynamic stability, showing that, as electron energy increases, the temperature correspondingly rises. Therefore, applying Tsallis entropy with $0 < q_T < 1$ is appropriate for this study's plasma system. Furthermore, this finding aligns with the principle of entropy increase associated with q-averaged energy. In contrast, the Rényi entropy with $q_R > 1$, which has been reported to fail in satisfying the condition of concavity, is regarded as physically unsuitable in the plasma system investigated in this study.

TABLE II. Effect of electric field on q-parameters in Tsallis and Rényi statistics. The test conditions are as follows: gas temperature $T_g = 0.026$ eV, electron density $n_e = 2 \times 10^{13}$ cm^{-3}, and ionization degree 0.012%, for reduced electric field range $1 \leqslant E/N$ [Td] $\leqslant 10$.

	Tsallis		Rényi	
E/N [Td]	q_T	$1/\beta$	q_R	$1/\beta$
1	0.913	1.68	1.085	1.55
2	0.880	2.15	1.118	1.92
3	0.862	2.40	1.134	2.10
4	0.854	2.55	1.145	2.25
5	0.845	2.70	1.154	2.35
6	0.835	2.85	1.160	2.45
7	0.833	2.90	1.163	2.50
8	0.832	2.95	1.165	2.55
9	0.825	3.10	1.170	2.65
10	0.818	3.15	1.178	2.70

C. Temperature based on nonextensive Tsallis and extensive Rényi statistics

Using Tsallis and Rényi statistics, we calculated several temperatures, as defined in Eqs. (10), (32), (33), (18), (34), and (35). The results in Fig. 7 confirm the relation $T_{\beta-\text{Tsallis}} = T_{q-\text{Tsallis}} = T_{U_q-\text{Tsallis}}$; the three temperatures derived for electrons in nonequilibrium plasma using Eqs. (10), (32), and (33) on Tsallis statistics coincide. Additionally, we confirm the relation $T_{\beta-\text{Rényi}} = T_{q-\text{Rényi}} = T_{U-\text{Rényi}}$; the three temperatures derived for electrons in nonequilibrium plasma using Eqs. (18), (34), and (35) on Rényi statistics also coincide. In addition, Fig. 7 illustrates the comparison between T_{Tsallis}, $T_{\text{Rényi}}$, and T_{low_E}, which is the temperature determined by the differential coefficient of the distribution function at $\epsilon = 0$ eV (obtained with values of 0 and 0.003 eV). The inequality $T_{\text{Tsallis}} > T_{\text{Rényi}}$ always holds due to T_{Tsallis} being determined by the q-average energy U_q with a power exponent less than 1. However, since the Rényi entropy fails to satisfy the property of concavity in $q_R > 1$ [90], it is deemed unsuitable as a physically meaningful entropy in this study's plasma system. Thus, the resulting Rényi temperature is nothing more than a hypothetical value derived through formal calculation.

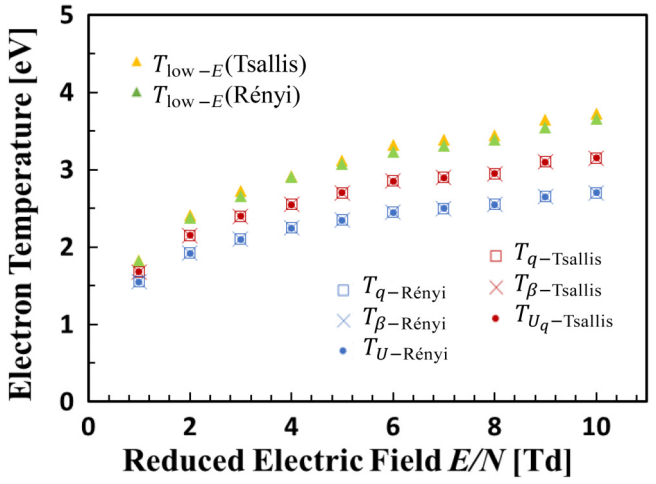

FIG. 7. Comparison between electron temperatures based on nonextensive Tsallis and extensive Rényi statistics plotted against reduced electric field.

Consequently, the Tsallis temperature derived from the Tsallis entropy, satisfying concavity in $0 < q_T < 1$, more effectively characterizes the features of this study's plasma system. Furthermore, T_{low_E} has the highest calculated temperature, as any distribution function has a larger slope than that of the differential coefficient of the distribution function at $\epsilon = 0\,\text{eV}$. Therefore, the temperature derived from Tsallis and Rényi statistics considers the curvilinear distribution of the high-energy tail, as opposed to that determined from the differential coefficient of the distribution function.

Given that the EEPF of the low-temperature weakly ionized plasma discussed in Sec. III A exhibits a power-law tail, it can be fitted by the Tsallis and Rényi distributions, and the Tsallis and Rényi temperatures are determined. However, in nonequilibrium plasma that evolves over time and exhibits a non-power-law tail, as exemplified by relativistic laser-induced physics [93] such as plasmas generated by relativistically intense and high-temporal-contrast femtosecond laser pulses, fitting with the Tsallis and Rényi distributions becomes inadequate. Nevertheless, nature favors distributions with power-law tails; indeed, numerical studies demonstrate that power-law tails are the intrinsic outcome of various dynamical processes, including phenomena such as magnetic reconnection [5,94,95], shock wave [6], plasma turbulence [96–98], and low-pressure gas discharge plasma [13,87]. Hence, these power-law distributions can represent various natural phenomena because they are derived from the principles of Tsallis and Rényi entropy maximization. This implies that the principle of entropy maximization is fundamental to numerical nonequilibrium phenomena in nature.

IV. CONCLUSION

This study investigated the temperature of out-of-equilibrium free electrons that deviate from the Maxwell-Boltzmann distribution, as documented in numerous observations. In nonequilibrium plasmas, the electron temperature cannot be uniquely determined using traditional Boltzmann-Gibbs statistics. Specifically, the electron temperature derived from the slope of the Boltzmann plot, which indicates temperature under the Gibbs entropy maximization principle, does not align with the partial derivative of entropy with respect to the mean energy. Moreover, the electron temperature derived from the mean energy cannot coexist within the framework of current conventional Boltzmann-Gibbs statistics. To overcome this problem, Tsallis and Rényi entropies were applied to nonequilibrium systems based on extensive and nonextensive statistical physics. This approach determined the electron temperature from a power-law distribution under the entropy maximization principle rather than an approximated exponential distribution in the Boltzmann plot. Thus, the electron temperature was uniquely determined: in nonequilibrium plasmas, the electron temperature derived from the partial derivative of entropy and the mean or q-average energy successfully coexist.

This may open additional research avenues, as current conventional methods for determining temperature often overlook the curvilinear distribution of the high-energy tail in plasma physics. Therefore, it is possible to describe more detailed properties of the plasma using the q parameter in addition to the temperature T based on the Tsallis and Rényi entropy maximization principles. When the limit $q \to 1$, traditional Gibbs entropy is exactly recovered, suggesting the unification of these different distributions encountered in nonequilibrium plasmas. Consequently, the ultimate goal of this study lies in several practical applications and discussions on physical phenomena in the world, by introducing additional parameters q that expand the meaning of temperature T. These enhancements enable a more precise and high-resolution representation of the application and nature of plasma using temperature T and the q parameter related to curvature. Therefore, it opens some perspectives for the application to various distribution functions in which the high-energy tail of these energy distribution becomes either rich or depleted. Possible application areas include plasma processing [99–101], plasma medicine [102,103], thermonuclear fusion [104–106], and space plasma [5,107]. Although our analysis focuses on plasmas containing a depleted high-energy component [13–19], there are potential applications in plasmas characterized by distribution functions that incorporate a rich high-energy component [5–12].

However, nonextensive statistical mechanics contain open problems [108]. Their physical significance remains undefined, although studies have been conducted based on superstatistics [11] and the derivation of q exponents and Tsallis entropy based on the number of weighted microstates of the phase space [34]. Furthermore, the constraint of requiring the same q parameter across multiple systems remains in place. Advancing the understanding of temperature in nonequilibrium systems requires resolving the existing unresolved issues.

ACKNOWLEDGMENTS

This study was supported by the Japan Society for the Promotion of Science (Grant No. 22K03566). The authors

thank Prof. Hiroaki Tsutsui and Prof. Jun Hasegawa of the Institute of Science Tokyo, for their discussions.

DATA AVAILABILITY

The data that support the findings of this article are openly available at [109].

[1] J. S. Rowlinson, The Maxwell–Boltzmann distribution, Mol. Phys. **103**, 2821 (2005).

[2] J. Y. Kim, H.-C. Lee, G. Go, Y. H. Choi, Y. S. Hwang, and K.-J. Chung, Exploring the nonextensive thermodynamics of partially ionized gas in magnetic field, Phys. Rev. E **104**, 045202 (2021).

[3] A. D. Oylukan and B. Shizgal, Nonequilibrium distributions from the Fokker-Planck equation: Kappa distributions and Tsallis entropy, Phys. Rev. E **108**, 014111 (2023).

[4] R. J. Ewart, M. L. Nastac, and A. A. Schekochihin, Non-thermal particle acceleration and power-law tails via relaxation to universal Lynden-Bell equilibria, J. Plasma Phys. **89**, 905890516 (2023).

[5] M. Hoshino, T. Mukai, T. Terasawa, and I. Shinohara, Suprathermal electron acceleration in magnetic reconnection, J. Geophys. Res.: Space Phys. **106**, 25979 (2001).

[6] M. Hoshino and N. Shimada, Nonthermal electrons at high mach number shocks: Electron shock surfing acceleration, Astrophys. J. **572**, 880 (2002).

[7] S. Mochizuki, S. Mattei, K. Nishida, A. Hatayama, and J. Lettry, Numerical analysis of electron energy distribution function and its effects on the H^- production in Linac4 H^- source, Plasma Fusion Res. **11**, 2406044 (2016).

[8] O. Ishihara and A. Hirose, Quasilinear mechanism of high-energy ion-tail formation in the ion-acoustic instability, Phys. Rev. Lett. **46**, 771 (1981).

[9] C. Swanson, P. Jandovitz, and S. A. Cohen, Using Poisson-regularized inversion of Bremsstrahlung emission to extract full electron energy distribution functions from x-ray pulse-height detector data, AIP Adv. **8**, 025222 (2018).

[10] J. L. Reis, J. Amorim, and A. D. Pino, Rotational temperature measurements in molecular plasmas using nonadditive Tsallis statistics, Physica A **404**, 192 (2014).

[11] K. Ourabah, Demystifying the success of empirical distributions in space plasmas, Phys. Rev. Res. **2**, 023121 (2020).

[12] K. Takahashi, C. Charles, and R. W. Boswell, Enhanced diamagnetism by energetic tail electrons in a magnetized plasma, Phys. Rev. Res. **5**, L022029 (2023).

[13] M. J. Druyvesteyn and F. M. Penning, The mechanism of electrical discharges in gases of low pressure, Rev. Mod. Phys. **12**, 87 (1940).

[14] T. Fujimoto, Kinetics of Ionization-Recombination of a plasma and population density of excited ions. I. Equilibrium plasma, J. Phys. Soc. Jpn. **47**, 265 (1979).

[15] T. Fujimoto, Kinetics of ionization-recombination of a plasma and population density of excited ions. II. ionizing plasma, J. Phys. Soc. Jpn. **47**, 273 (1979).

[16] H. Akatsuka and M. Suzuki, Stationary population inversion of hydrogen in an arc-heated magnetically trapped expanding hydrogen-helium plasma jet, Phys. Rev. E **49**, 1534 (1994).

[17] H.-C. Lee and C.-W. Chung, Effect of electron energy distribution on the hysteresis of plasma discharge: Theory, experiment and modeling, Sci. Rep. **5**, 15254 (2015).

[18] K. Takahashi, C. Charles, R. W. Boswell, and T. Fujiwara, Electron energy distribution of a current-free double layer: Druyvesteyn theory and experiments, Phys. Rev. Lett. **107**, 035002 (2011).

[19] H. Onishi, F. Yamazaki, Y. Hakozaki, M. Takemura, A. Nezu, and H. Akatsuka, Measurement of electron temperature and density of atmospheric-pressure non-equilibrium argon plasma examined with optical emission spectroscopy, Jpn. J. Appl. Phys. **60**, 026002 (2021).

[20] N. Ohno, M. A. Razzak, H. Ukai, S. Takamura, and Y. Uesugi, Validity of electron temperature measurement by using Boltzmann plot method in radio frequency inductive discharge in the atmospheric pressure range, Plasma Fusion Res. **1**, 028 (2006).

[21] H. Akatsuka, Optical emission spectroscopic (OES) analysis for diagnostics of electron density and temperature in non-equilibrium argon plasma based on collisional-radiative model, Adv. Phys. X **4**, 1592707 (2019).

[22] T. Völker and I. B. Gornushkin, Importance of physical units in the Boltzmann plot method, J. Anal. At. Spectrom. **37**, 1972 (2022).

[23] R. Zgadzaj, J. Welch, Y. Cao, L. D. Amorim, A. Cheng, A. Gaikwad, P. Iapozzutto, P. Kumar, V. N. Litvinenko, I. Petrushina, R. Samulyak, N. Vafaei-Najafabadi, C. Joshi, C. Zhang, M. Babzien, M. Fedurin, R. Kupfer, K. Kusche, M. A. Palmer, I. V. Pogorelsky *et al.*, Plasma electron acceleration driven by a long-wave-infrared laser, Nat. Commun. **15**, 4037 (2024).

[24] I. B. Denysenko, H. Kersten, and N. A. Azarenkov, Electron energy distribution function, effective electron temperature, and dust charge in the temporal afterglow of a plasma, Phys. Plasmas **23**, 053704 (2016).

[25] U. Kortshagen, A. Shivarova, E. Tatarova, and D. Zamfirov, Electron energy distribution function in a microwave discharge created by propagating surface waves, J. Phys. D: Appl. Phys. **27**, 301 (1994).

[26] S. F. Adams, J. A. Miles, and V. I. Demidov, Non-Maxwellian electron energy distribution function in a pulsed plasma modeled with dual effective temperatures, Phys. Plasmas **24**, 053508 (2017).

[27] V. A. Godyak and V. I. Demidov, Probe measurements of electron-energy distributions in plasmas: What can we measure and how can we achieve reliable results? J. Phys. D: Appl. Phys. **44**, 233001 (2011).

[28] R. Alvarez, J. Cotrino, and A. Palmero, On the kinetic and thermodynamic electron temperatures in non-thermal plasmas, Europhys. Lett. **105**, 15001 (2014).

[29] H. Akatsuka and Y. Tanaka, Discussion on electron temperature of gas-discharge plasma with non-Maxwellian electron energy distribution function based on entropy and statistical physics, Entropy **25**, 276 (2023).

[30] K. Kikuchi and H. Akatsuka, Reconsideration of temperature determined by the excited-state population distribution of

Hydrogen atoms based on Tsallis entropy and its statistics in hydrogen plasma in non-equilibrium state, Entropy **25**, 1400 (2023).

[31] C. Tsallis, *Introduction to Nonextensive Statistical Mechanics: Approaching a Complex World* (Springer, New York, 2009).

[32] C. Tsallis, Possible generalization of Boltzmann-Gibbs statistics, J. Stat. Phys. **52**, 479 (1988).

[33] A. Rényi, On Measures of Entropy and Information, in *Proceedings of the Fourth Berkeley Symposium on Mathematical Statistics and Probability, Volume 1: Contributions to the Theory of Statistics* (University of California Press, Berkeley, CA, 1961), Vol. 4.1, pp. 547–562.

[34] V. García-Morales and J. Pellicer, Microcanonical foundation of nonextensivity and generalized thermostatistics based on the fractality of the phase space, Physica A **361**, 161 (2006).

[35] G. Kaniadakis, Non-linear kinetics underlying generalized statistics, Physica A **296**, 405 (2001).

[36] C. Beck and E. G. D. Cohen, Superstatistics, Physica A **322**, 267 (2003).

[37] K. Ourabah, L. Ait Gougam, and M. Tribeche, Nonthermal and suprathermal distributions as a consequence of superstatistics, Phys. Rev. E **91**, 012133 (2015).

[38] S. Davis, G. Avaria, B. Bora, J. Jain, J. Moreno, C. Pavez, and L. Soto, Single-particle velocity distributions of collisionless, steady-state plasmas must follow superstatistics, Phys. Rev. E **100**, 023205 (2019).

[39] R. A. Treumann and C. H. Jaroschek, Gibbsian theory of power-law distributions, Phys. Rev. Lett. **100**, 155005 (2008).

[40] B. M. Boghosian, Thermodynamic description of the relaxation of two-dimensional turbulence using Tsallis statistics, Phys. Rev. E **53**, 4754 (1996).

[41] C. Beck, G. S. Lewis, and H. L. Swinney, Measuring nonextensitivity parameters in a turbulent Couette-Taylor flow, Phys. Rev. E **63**, 035303(R) (2001).

[42] C. Tsallis, J. C. Anjos, and E. P. Borges, Fluxes of cosmic rays: A delicately balanced stationary state, Phys. Lett. A **310**, 372 (2003).

[43] G. P. Pavlos, A. C. Iliopoulos, V. G. Tsoutsouras, D. V. Sarafopoulos, D. S. Sfiris, L. P. Karakatsanis, and E. G. Pavlos, First and second order non-equilibrium phase transition and evidence for non-extensive Tsallis statistics in Earth's magnetosphere, Physica A **390**, 2819 (2011).

[44] A. Guha and P. K. Das, An extensive study of Bose–Einstein condensation in liquid helium using Tsallis statistics, Physica A **497**, 272 (2018).

[45] L. Enciso, M. Gun, M. S. Ruiz, and A. C. Razzitte, Entropy in multifractal non equilibrium structures of dielectric breakdown, J. Stat. Mech. (2019) 094011.

[46] A. Boumali, F. Serdouk, and S. Dilmi, Superstatistical properties of the one-dimensional Dirac oscillator, Physica A **553**, 124207 (2020).

[47] A. Chakraborty and R. Sensarma, Nonequilibrium dynamics of Renyi entropy for bosonic many-particle systems, Phys. Rev. Lett. **127**, 200603 (2021).

[48] M. Dheepika, H. B. V. T, and T. K. Mathew, Emergence of cosmic space in Tsallis modified gravity from equilibrium and non-equilibrium thermodynamic perspective, Phys. Scr. **99**, 015014 (2024).

[49] J. D'Emidio, Entanglement entropy from nonequilibrium work, Phys. Rev. Lett. **124**, 110602 (2020).

[50] V. Eisler, Entanglement negativity in a nonequilibrium steady state, Phys. Rev. B **107**, 075157 (2023).

[51] T. Arimitsu and N. Arimitsu, Analysis of turbulence by statistics based on generalized entropies, Physica A **295**, 177 (2001).

[52] V. Alba and P. Calabrese, Quench action and Rényi entropies in integrable systems, Phys. Rev. B **96**, 115421 (2017).

[53] S. Bhattacharyya, M. Haiduc, A. T. Neagu, and E. Firu, An investigation of Renyi entropy in high-energy nucleus–nucleus collisions, Can. J. Phys. **95**, 715 (2017).

[54] M. Niknam, L. F. Santos, and D. G. Cory, Experimental detection of the correlation Rényi entropy in the central spin model, Phys. Rev. Lett. **127**, 080401 (2021).

[55] V. Zhdankin, Non-thermal particle acceleration from maximum entropy in collisionless plasmas, J. Plasma Phys. **88**, 175880303 (2022).

[56] C. Tsallis, RenioS. Mendes, and A. R. Plastino, The role of constraints within generalized nonextensive statistics, Physica A **261**, 534 (1998).

[57] H. Suyari, The unique non-self-referential q-canonical distribution and the physical temperature derived from the maximum entropy principle in Tsallis statistics, Prog. Theor. Phys. Suppl. **162**, 79 (2006).

[58] S. Abe, S. Martínez, F. Pennini, and A. Plastino, Nonextensive thermodynamic relations, Phys. Lett. A **281**, 126 (2001).

[59] A. G. Bashkirov, Maximum Renyi entropy principle for systems with power-law Hamiltonians, Phys. Rev. Lett. **93**, 130601 (2004).

[60] A. G. Bashkirov, Renyi entropy as a statistical entropy for complex systems, Theor. Math. Phys. **149**, 1559 (2006).

[61] A. M. Scarfone, H. Matsuzoe, and T. Wada, A study of Rényi entropy based on the information geometry formalism, J. Phys. A: Math. Theor. **53**, 145003 (2020).

[62] G. J. Boyle, P. W. Stokes, R. E. Robson, and R. D. White, Boltzmann's equation at 150: Traditional and modern solution techniques for charged particles in neutral gases, J. Chem. Phys. **159**, 024306 (2023).

[63] G. J. M. Hagelaar and L. C. Pitchford, Solving the Boltzmann equation to obtain electron transport coefficients and rate coefficients for fluid models, Plasma Sources Sci. Technol. **14**, 722 (2005).

[64] L. L. Alves, The IST-LISBON database on LXCat, J. Phys.: Conf. Ser. **565**, 012007 (2014).

[65] O. Zatsarinny, BSR: B-spline atomic R-matrix codes, Comput. Phys. Commun. **174**, 273 (2006).

[66] O. Zatsarinny and K. Bartschat, The B-spline R-matrix method for atomic processes: Application to atomic structure, electron collisions and photoionization, J. Phys. B: At. Mol. Opt. Phys. **46**, 112001 (2013).

[67] Á. Yanguas-Gil, J. Cotrino, and L. L. Alves, An update of argon inelastic cross sections for plasma discharges, J. Phys. D: Appl. Phys. **38**, 1588 (2005).

[68] C. Yamabe, S. J. Buckman, and A. V. Phelps, Measurement of free-free emission from low-energy-electron collisions with Ar, Phys. Rev. A **27**, 1345 (1983).

[69] M. A. Khakoo, P. Vandeventer, J. G. Childers, I. Kanik, C. J. Fontes, K. Bartschat, V. Zeman, D. H. Madison, S. Saxena, R. Srivastava, and A. D. Stauffer, Electron impact excitation of the argon $3p^5 4s$ configuration: Differential cross-sections and cross-section ratios, J. Phys. B: At. Mol. Opt. Phys. **37**, 247 (2004).

[70] J. E. Chilton, J. B. Boffard, R. S. Schappe, and C. C. Lin, Measurement of electron-impact excitation into the $3p^5 4p$ levels of argon using Fourier-transform spectroscopy, Phys. Rev. A **57**, 267 (1998).

[71] T. Weber, J. B. Boffard, and C. C. Lin, Electron-impact excitation cross sections of the higher argon $3p^5 np$ ($n = 5,6,7$) levels, Phys. Rev. A **68**, 032719 (2003).

[72] H. W. Drawin, *Collision and Transport Cross-Sections*, Tech. Rep. No. EUR-CEA-FC-383(Rev.) (European Atomic Energy Community, Commissariat à l'Energie Atomique, Centre d'Etudes Nucléaires, Fontenay-aux-Roses, France, 1966).

[73] C.-M. Lee and K. T. Lu, Spectroscopy and collision theory. II. The Ar absorption spectrum, Phys. Rev. A **8**, 1241 (1973).

[74] J. Bretagne, G. Callede, M. Legentil, and V. Puech, Relativistic electron-beam-produced plasmas. I. Collision cross sections and loss function in argon, J. Phys. D: Appl. Phys. **19**, 761 (1986).

[75] J. Bretagne, J. Godart, and V. Puech, Low-energy electron distribution in an electron-beam-generated argon plasma, J. Phys. D: Appl. Phys. **15**, 2205 (1982).

[76] D. Rapp and P. Englander-Golden, Total cross sections for ionization and attachment in gases by electron impact. I. Positive ionization, J. Chem. Phys. **43**, 1464 (1965).

[77] T. Holstein, Energy distribution of electrons in high frequency gas discharges, Phys. Rev. **70**, 367 (1946).

[78] R. Winkler, H. Deutsch, J. Wilhelm, and Ch. Wilke, Electron Kinetics of weakly ionized HF plasmas I. Direct treatment and fourier expansion, Beitr. Plasmaphys. **24**, 285 (1984).

[79] R. Winkler, H. Deutsch, J. Wilhelm, and Ch. Wilke, Electron kinetics of weakly ionized HF plasmas. II. Decoupling in the fourier hierarchy and simplified kinetics at higher frequencies, Beitr. Plasmaphys. **24**, 303 (1984).

[80] P. K. Tiwari, R. Kumar, K. Halder, and Y. S. Lee, Maxwell–Boltzmann and Druyvesteyn distribution functions expressing the particle velocity and the energy in sheath plasmas, J. Russ. Laser Res. **44**, 504 (2023).

[81] I. B. Denysenko, N. A. Azarenkov, K. Ostrikov, and M. Y. Yu, Electron energy probability function in the temporal afterglow of a dusty plasma, Phys. Plasmas **25**, 013703 (2018).

[82] J. T. Gudmundsson, On the effect of the electron energy distribution on the plasma parameters of an argon discharge: A global (volume-averaged) model study, Plasma Sources Sci. Technol. **10**, 76 (2001).

[83] J. B. Boffard, R. O. Jung, C. C. Lin, and A. E. Wendt, Optical emission measurements of electron energy distributions in low-pressure argon inductively coupled plasmas, Plasma Sources Sci. Technol. **19**, 065001 (2010).

[84] C. E. Shannon, A mathematical theory of communication, Bell Syst. Tech. J. **27**, 379 (1948).

[85] H. Suyari and M. Tsukada, Tsallis differential entropy and divergences derived from the generalized Shannon-Khinchin axioms, in *Proceedings of the 2009 IEEE International Symposium on Information Theory* (IEEE, New York, 2009), pp. 149–153.

[86] T. van Erven and P. Harremos, Rényi Divergence and Kullback-Leibler Divergence, IEEE Trans. Inf. Theory **60**, 3797 (2014).

[87] Y. Shimizu, Y. Kittaka, A. Nezu, H. Matsuura, and H. Akatsuka, Excited state distributions of hydrogen atoms in the microwave discharge hydrogen plasma and the effect of electron energy probabilistic function, IEEE Trans. Plasma Sci. **43**, 1758 (2015).

[88] K. Kano, M. Suzuki, and H. Akatsuka, Spectroscopic measurement of electron temperature and density in argon plasmas based on collisional-radiative model, Plasma Sources Sci. Technol. **9**, 314 (2000).

[89] K. Kuwano, A. Nezu, H. Matsuura, and H. Akatsuka, Dissociation degree of nitrogen molecule in low-pressure microwave-discharge nitrogen plasma with various rare-gas admixtures, Jpn. J. Appl. Phys. **55**, 086101 (2016).

[90] T. Wada, On the thermodynamic stability conditions of Tsallis' entropy, Phys. Lett. A **297**, 334 (2002).

[91] O. Kaburaki, Should entropy be concave? Phys. Lett. A **185**, 21 (1994).

[92] J. R. Rygg, P. M. Celliers, and G. W. Collins, Specific heat of electron plasma waves, Phys. Rev. Lett. **130**, 225101 (2023).

[93] Z. Samsonova, S. Höfer, V. Kaymak, S. Ališauskas, V. Shumakova, A. Pugžlys, A. Baltuška, T. Siefke, S. Kroker, A. Pukhov, O. Rosmej, I. Uschmann, C. Spielmann, and D. Kartashov, Relativistic interaction of long-wavelength ultrashort laser pulses with nanowires, Phys. Rev. X **9**, 021029 (2019).

[94] L. Sironi and A. Spitkovsky, Relativistic reconnection: An efficient source of non-thermal particles, Astrophys. J. **783**, L21 (2014).

[95] G. R. Werner and D. A. Uzdensky, Reconnection and particle acceleration in three-dimensional current sheet evolution in moderately magnetized astrophysical pair plasma, J. Plasma Phys. **87**, 905870613 (2021).

[96] M. W. Kunz, J. M. Stone, and E. Quataert, Magnetorotational turbulence and dynamo in a collisionless plasma, Phys. Rev. Lett. **117**, 235101 (2016).

[97] V. Zhdankin, G. R. Werner, D. A. Uzdensky, and M. C. Begelman, Kinetic turbulence in relativistic plasma: From thermal bath to nonthermal continuum, Phys. Rev. Lett. **118**, 055103 (2017).

[98] L. Comisso and L. Sironi, Particle acceleration in relativistic plasma turbulence, Phys. Rev. Lett. **121**, 255101 (2018).

[99] M. J. Kushner, A model for the discharge kinetics and plasma chemistry during plasma enhanced chemical vapor deposition of amorphous silicon, J. Appl. Phys. **63**, 2532 (1988).

[100] P. L. G. Ventzek, R. J. Hoekstra, and M. J. Kushner, Two-dimensional modeling of high plasma density inductively coupled sources for materials processing, J. Vac. Sci. Technol. B **12**, 461 (1994).

[101] Y. Yamashita, T. Akiba, T. Iwanaga, S. Date, H. Yamaoka, and H. Akatsuka, Optical emission spectroscopic measurement of argon low-pressure inductively coupled plasma based on the optimization algorithm of plasma diagnostic model, IEEE Trans. Plasma Sci. **50**, 1875 (2022).

[102] G. Fridman, G. Friedman, A. Gutsol, A. B. Shekhter, V. N. Vasilets, and A. Fridman, Applied plasma medicine, Plasma Process. Polym. **5**, 503 (2008).

[103] M. G. Kong, G. Kroesen, G. Morfill, T. Nosenko, T. Shimizu, J. van Dijk, and J. L. Zimmermann, Plasma medicine: An introductory review, New J. Phys. **11**, 115012 (2009).

[104] S. Ding, A. M. Garofalo, H. Q. Wang, D. B. Weisberg, Z. Y. Li, X. Jian, D. Eldon, B. S. Victor, A. Marinoni, Q. M. Hu, I. S. Carvalho, T. Odstrčil, L. Wang, A. W. Hyatt, T. H. Osborne, X. Z. Gong, J. P. Qian, J. Huang, J. McClenaghan, C. T. Holcomb *et al.*, A high-density and high-confinement tokamak plasma regime for fusion energy, Nature (London) **629**, 555 (2024).

[105] T. K. Popov, P. Ivanova, J. Stöckel, and R. Dejarnac, Electron energy distribution function, plasma potential and electron density measured by Langmuir probe in tokamak edge plasma, Plasma Phys. Control. Fusion **51**, 065014 (2009).

[106] T. S. V. K. Popov, M. Dimitrova, M. A. Pedrosa, D. López-Bruna, J. Horacek, J. Kovačič, R. Dejarnac, J. Stöckel, M. Aftanas, P. Böhm, P. Bílková, C. Hidalgo, and R. Panek, Bi-Maxwellian electron energy distribution function in the vicinity of the last closed flux surface in fusion plasma, Plasma Phys. Control. Fusion **57**, 115011 (2015).

[107] M. Oka, J. Birn, M. Battaglia, C. C. Chaston, S. M. Hatch, G. Livadiotis, S. Imada, Y. Miyoshi, M. Kuhar, F. Effenberger, E. Eriksson, Y. V. Khotyaintsev, and A. Retinò, Electron power-law spectra in solar and space plasmas, Space Sci. Rev. **214**, 82 (2018).

[108] K. P. Nelson, Open problems within nonextensive statistical mechanics, Entropy **26**, 118 (2024).

[109] https://github.com/kknu5656/Physical-Review-E-data.